Lawrence Berkeley National Laboratory
Recent Work

Title

THEORETICAL STUDY OF TWO NUCLEON TRANSFER BETWEEN HEAVY IONS INCLUDING THE EFFECT OF INELASTIC PROCESSES

Permalink

https://escholarship.org/uc/item/762626w3

Authors

Glendenning, Norman K.
Ascuitto, R.J.

Publication Date

1973-03-01

THEORETICAL STUDY OF TWO NUCLEON TRANSFER
BETWEEN HEAVY IONS INCLUDING THE
EFFECT OF INELASTIC PROCESSES

Norman K. Glendenning and R. J. Ascuitto

March 1973

DISCLAIMER

THEORETICAL STUDY OF TWO NUCLEON TRANSFER BETWEEN HEAVY IONS INCLUDING THE EFFECT OF INELASTIC PROCESSES[*]

Norman K. Glendenning
Lawrence Berkeley Laboratory

R. J. Ascuitto[†]
Niels Bohr Institute

Although by now many experiments involving the transfer of one or several nucleons between heavy ions have been carried out, there remain unsettled questions concerned with the mechanism of these reactions. Do second order processes involving the inelastic excitation of the target or residual nucleus play an important role in the reaction? To date such theoretical analyses as have been carried out assume that they do not. The distorted wave Born approximation (DWBA) has been used to compute the direct transfer contribution and there is no strong disagreement with experiment to suggest that this approach is inadequate. However, from our earlier work on reactions induced by light nuclides, such as (p,t) and (d,p), we do know that the higher order processes mentioned above are sometimes very important.[1] The fact that in Coulomb excitation experiments, collective states are produced with probability approaching unity suggests to us that they ought to be important in heavy ion reactions also.

Here we report a study of the reaction $^{120}Sn(^{18}O,^{16}O)^{122}Sn$ at 100 MeV, designed to estimate the effects produced on the cross sections of particle transfer reactions at around 100 MeV of higher order processes shown in Fig. 1. Our method of doing this type of calculation is the so-called source term method which we have developed in earlier publications.[2] The usual DWBA treats only a single transition for each state, namely that from the target ground state to the residual state of the product nucleus.
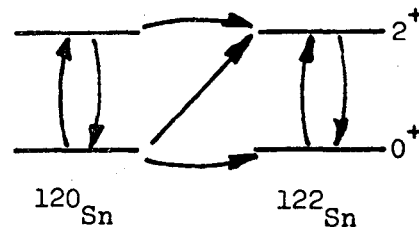

Fig. 1

We describe briefly the nature of the structure of the nuclei which is relevant to this reaction. The ground state of ^{18}O is treated as an inert

core of ^{16}O plus two neutrons which may occupy the $s_{1/2}$, $d_{3/2}$ and $d_{5/2}$ orbitals in a Woods-Saxon potential which binds them at approximately the energies observed in ^{17}O. The interaction matrix elements between pairs of neutrons in each of these configurations is assumed to be of the pairing force type of such a strength that the binding energy of the last two neutrons is correct. Two states of each tin nucleus are included, the ground and the collective 2^+ state. The former is described as a BCS vacuum state, and the latter as a collective two-quasiparticle state. The neutron orbitals of Sn are generated from a Woods-Saxon potential corresponding to the average parameters of Myers.[3] The form factor for the transfer of two nucleons based on these nuclear descriptions is shown in Fig. 2. The projected wave function, or form factor, is more complicated to obtain than in (t,p) reactions, because of the necessity to retain the finite range of the interactions. It is defined by the following identity for transfer from the pure configuration $(j^2)0$ in the projectile to the configuration $(j_1 j_2)J$ in the residual nucleus:

$$\iint d\underset{\sim}{r}_1\, d\underset{\sim}{r}_2\, \psi_{(j_1 j_2)J}^{M}{}^{*}(\underset{\sim}{r}_1',\underset{\sim}{r}_2')\, \{V(r_1) + V(r_2)\}\, \psi_{(j^2)0}(\underset{\sim}{r}_1,\underset{\sim}{r}_2)$$

$$\equiv U_J(R)\, Y_J^{M}{}^{*}(\hat{R}) \tag{1}$$

Here V is the Woods-Saxon potential which binds the neutrons in ^{18}O, $\underset{\sim}{R}$ is the vector joining the core of the projectile (^{16}O) to the target nucleus (^{120}Sn), $\underset{\sim}{r}_1$ and $\underset{\sim}{r}_2$ are the coordinates of the two neutrons with respect to the projectile core, while $\underset{\sim}{r}_1'$ and $\underset{\sim}{r}_2'$ are their coordinates with respect to the target nucleus.

$$\underset{\sim}{r}_1' = \underset{\sim}{r}_1 + \underset{\sim}{R} \tag{2}$$

For mixed configurations such as we use, and are illustrated in Fig. 2, the form factor is obtained by weighting such form factors by the product of parentage amplitudes for the light and heavy nuclei involved. We note from Fig. 2 that the J = 0 form factor is considerably bigger than the J = 2. For this reason, we include only the monopole transition connecting the 2^+ states in Fig. 1, although in principle they can be connected by J = 2 and 4 as well. The reduction of the left side of Eq. (1) to a form suitable for

numerical computation of the form factor $U_J(R)$ is complicated and we do not discuss it here.

Recoil effects are neglected. We do not believe that this neglect can effect our estimate of the importance of higher order processes compared to the direct transition, although in a detailed comparison with experiment it may well be important to include recoil effects.[4]

The inelastic transitions are computed on the basis of the macroscopic vibrational model. The nuclear deformation parameter β_2 for the tin isotopes are taken from an analysis of proton scattering.[5] We use the same optical model parameters as Becchetti et al.[6] in their analysis of $^{16}O + ^{208}Pb$ scattering. These authors find the deformation parameter obtained in proton experiments consistent with their determination in the heavy ion experiment. For this reason we can have considerable confidence in our estimate of the strength of the inelastic processes. We determine the strength of the Coulomb quadrupole term in the interaction by using the experimentally determined[7] value of B(E2). The nuclear and charge deformation are shown in Table I. The nuclear field is deformed according to

$$V[r - R(\theta)] = V(r - R) - \beta_2 R_T \frac{\partial V}{\partial r} Y_2(\theta)$$

where

$$R(\theta) = R_P + R_T[1 + \beta_2 Y_{20}(\theta)]$$

corresponding to a spherical projectile of "radius" R_P and a vibrational target of radius R_T. Of course it is $R_P + R_T$ which is to be identified with the optical model radius which is typically parameterized as $r_0(A_P^{1/3} + A_T^{1/3})$. It is the product $\beta_2 R_T$ which is determined for us by the proton scattering experiment while the sum $R_P + R_T$ is determined by the analysis of heavy ion elastic scattering. We have relied upon an extrapolation of the optical potential from Pb to Sn. We checked this by using an alternative potential determined by Morrison[8] for $^{16}O + ^{48}Ca$. These two rather different parameterizations are shown in Table II. They yield cross sections which are virtually the same and this gives us confidence that the results presented below do not contain any uncertainty attributable to optical model parameters or deformation.

Of course in a calculation such as this, the relative phase between inelastic and particle transfer form factors must be preserved when the inelastic scattering is computed from a macroscopic parameterization.

Our first calculation shown in Fig. 3 shows the cross sections for the ground and 2^+ state of tin produced in the reaction

$$^{18}O + ^{120}Sn \rightarrow ^{16}O + ^{122}Sn$$
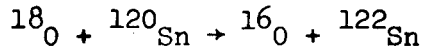
with 100 MeV oxygen ions. (The Coulomb barrier is around 60 MeV.) The calculations employ the conventional distorted wave Born approximation. We see the characteristic maxima occuring at what is referred to as the grazing angle, in this case, about 38°. If indeed the oxygen ion followed a strictly Coulomb orbit, the distance of closest approach is in this case 13.5 F. Actually because of the nuclear attraction we expect that to the extent that a given scattering angle can be associated with a well defined orbit, its closest approach would be less than this. Indeed if we set the form factor equal to zero beyond 12 F the cross sections are not much reduced (but they are strongly modified in angular shape).

The result of a coupled channel calculation which includes the effects of inelastic excitation of the tin nuclei via the routes of Fig. 1 is shown in Fig. 4. The ground state is barely altered so we show no comparison, but the 2^+ state is strongly effected by the additional modes of excitation. In particular, the direct transition shown by a dashed line, interferes destructively with the indirect modes of excitation and produces an angular distribution in which the expected peak at the grazing angle is absent. Instead a poor angular resolution experiment would observe a monotonically decreasing distribution, fairly flat at first, and then falling rapidly after the grazing angle, or peak in the ground state cross section. This is in marked contrast with the DWBA prediction. Of course there is a continuous evolution from the dashed curve to the solid, as a function of deformation constants β, or collectivity of the intermediate states. As remarked earlier, we determined the appropriate values from other experiments, and such values, listed in Table I, were used in the calculation shown in Fig. 4. The effect of increasing the deformation by $\sqrt{2}$ and 2, corresponding approximately to doubling and quadrupling the inelastic cross section to the 2^+ state is shown in Fig. 5 by the solid lines. The dotted curve corresponds to the correct tin

deformation constants shown for comparison and are reproductions of Fig. 4.
In the 2^+ cross section, we see a progressively deeper dip occuring at the
grazing angle, because of the destructive interference between the direct
amplitude which is peaked at the grazing angle (Fig. 4) and the indirect
amplitudes which are growing about linearly with increasing collectivity. At
the same time a peak grows, proportional to the increasing collectivity, at
an angle of about 10° beyond the grazing angle, which belongs to the indirect
amplitudes. We here see how   the peak of the cross section near the
grazing angle can be shifted relative to other levels in a given nucleus, or
relative to the analogous level in a neighboring nucleus. We add that the
broadening of the whole angular distribution structure of the 2^+ state which
is produced by the indirect amplitudes, has its origin in the broader peak of
the inelastic angular distributions compared to the direct particle transfer.
This difference in turn corresponds to the sharper confinement of the transfer
process by the exponential decay of bound state wave functions.

In contrast to the 2^+ state, the ground state cross section is little
effected in the vicinity of the grazing angle but the fall-off toward forward
angles is accelerated at the higher collectivity. Unlike the 2^+, the ground
state is dominated by the direct amplitude.

Although the Coulomb central field is crucial in determining the general
features of the cross sections, the Coulomb contribution to the higher order
transitions turns out to be small (and of opposite sign) compared to the
contribution of the nuclear field. In Fig. 6 the results of a calculation in
which the higher intermediate states are produced only by Coulomb excitation
are compared with the DWBA. We see that the coupling changes the 2^+ state
most, by a 15% increase in cross sections at the grazing angle. This,
however, is in marked contrast to a reduction in cross section by a factor of
4 when the nuclear excitation is included, as we saw in Fig. 4. Moreover, the
strong forward cross section produced by nuclear excitations is not duplicated
by the Coulomb excitation alone.

The Q value of this reaction is 2.8 MeV. It is interesting to know how
the balance between direct and indirect amplitudes depends on Q, since as is
well known, the magnitude of the cross sections depend strongly on the Q. In
Fig. 7 we show what would result if the Q had the less favorable value of
-6 MeV. Comparing with Fig. 4 we see that the ground state cross section and
the direct cross section to the 2^+ state have fallen by a factor of about 50,

while the complete 2^+ cross section has fallen only by about a factor of 30.
From this comparison we learn that, other things being similar, an unfavorable
Q value emphasizes the contribution of higher order transitions in particle
transfer reactions. Also note that the angular distribution of the 2^+ state
has changed considerably in comparison with Fig. 4 because of a change in the
shape of the indirect amplitudes.

To illustrate the dependence of the angular distribution on the Q value
we compare in Fig. 8 two calculations corresponding to Q = ±6 MeV. We note the
marked change in angular distribution of the 2^+ state. Note also that the
magnitudes are reduced strongly for Q = -6 showing that the optimum Q is not
zero for this chargeless exchange.

At this point we remark on the unusual high frequency ripples that appear
at forward scattering angles, and are damped out toward larger angles. These
owe their origin to the fact that the heavy ion cross section for transfer of
nucleons is dominated by a fairly narrow band of partical waves (about 20 say)
centered at a high ℓ value of about 60 for this reaction at 100 MeV. We are
seeing essentially the distribution of $\ell = 60$ and its near neighbors, which are
close to being in phase at $\theta = 0$. In the less favorable $\theta = -6$ MeV case, the
spread in relevant partial waves is broader, and consequently the ripples are
damped faster. The localization in ℓ is associated with a reaction ring,
bounded on the inner side by absorption, and on the outer by the exponential
decay of bound state wave functions. For inelastic scattering, especially to
collective states, the outer edge of the ring is very diffuse, and indeed
because of the slow fall off of the electric multiple fields can hardly be
said to exist.

Now we mention an interesting feature of the interference between the
direct and indirect routes which, we have noted, is _destructive_ at the grazing
angle. We recall that, to lowest order, the interaction causing inelastic
transitions is

$$V_2 \simeq \left[-\beta_2 R \frac{\partial V}{\partial r} + \sqrt{\frac{\pi}{5}} \frac{Z'e^2 Q_0}{r^3} \right] Y_2(\theta) \quad , \quad r > R_c$$

Now in spherical nuclei, where β_2 measures the amplitude of vibrations away
from spherical shape, no meaning attaches to a negative sign. However, for
permanently deformed, nuclei, a negative β_2 has meaning and corresponds to an
oblate nucleus. In this case the sign of the amplitudes of the indirect
routes would interfere <u>constructively</u> with the direct route in contrast to
prolate deformed nuclei and spherical vibrational nuclei. Figure 9 shows the
result of such a change in sign and can be compared to the normal situation
for spherical nuclei.

Now we turn to the question of energy dependence. At 80 MeV, as shown
in Fig. 10, the interference between the direct and indirect transition
produces a shallow depression at the grazing angle in the 2^+ cross section
which produces a maximum at an angle about 6° less than the grazing angle.
At 120 MeV as seen in Fig. 11, the 2^+ cross section bears even less resemblance
to the expected distribution peaked at the grazing angle, as the ground state
cross section is. The jagged spikes occuring beyond 60° are of course not
physical. We show them to illustrate an effect of a too early truncation in
ℓ. All calculations shown were performed with 100 partial waves, although
the first 30 or so make no contribution at these energies. By also performing
a calculation with ℓ_{max} = 90 we can check to see in what angular region
differences occur from the full calculation using ℓ_{max} = 99. We found that
this upper limit yields convergence in the cross section for $\theta \lesssim 55°$ at
E = 120 MeV, for $\theta \lesssim 70°$ at E = 100 MeV, and for E = 80 MeV, over the whole
forward hemisphere.

There remains much to be done in clarifying the details of the reaction
mechanism. We can conclude from this work, so far, that the usual first order
treatment of heavy ion transfer reactions is often inadequate and that the
higher order processes involving the excitation of the target or residual
nucleus are essential for a correct description. Moreover, by examining Fig.
1 and 2 it is easy to understand why the indirect routes are negligible compared
to the direct for the 0^+ state, while they can be important for the 2^+ state.
We hypothesize therefore that all collective states receive a large second
order contribution from the branches

$$O(A) \rightarrow J(A) \rightarrow J(A + 2) \quad \text{and} \quad O(A) \rightarrow O(A + 2) \rightarrow J(A + 2)$$

in which the nucleon transfer segment goes by a monopole transition. We
qualified our rule to hold for collective states, since these are the only

ones for which the monopole segment will be analogous if not identical to the

$O(A) \rightarrow O(A + 2)$ transition (and hence stronger than the direct $O(A) \rightarrow J(A + 2)$).

We found the effect of the higher order processes was to destroy the
simple distribution consisting of a peak at the grazing angle that is expected
from classical considerations. Moreover the precise effect is obviously a
strong function of the collectivity of the intermediate state, but not so
obviously, also of the Q of the reaction. Because of the destructive interference
between direct and indirect amplitudes, the resulting angular distributions are
expected to show considerable variation from level to level and from nucleus to
nucleus.

References

1. R. J. Ascuitto and N. K. Glendenning, Phys. Rev. C2, 1260 (1970); R. J. Ascuitto, N. K. Glendenning and B. Sorensen, Phys. Rev. Letters, 34B, 17 (1971) and Nucl. Phys. A183, 60 (1972); N. K. Glendenning and R. S. Macintosh, Nucl. Phys. A168, 575 (1971).
2. R. J. Ascuitto and N. K. Glendenning, Phys. Rev. 181, 1396 (1969) and Nucl. Phys. A188, 185 (1972).
3. W. D. Myers, Nucl. Phys. A145, 387 (1970); Table I.
4. M. A. Nagarajan, Nucl. Phys. A196, 34 (1972).
5. O. Beer et al., Nucl. Phys. A147, 326 (1970); Table II and IX.
6. F. D. Becchetti et al., Phys. Rev. C6, 2215 (1972).
7. P. H. Stelson and L. Grodzins, Nuclear Data A1, 21 (1965).
8. G. C. Morrison, Journal de Physique 32, No. 11-12 (1971).

Table I. Nuclear and charge quadrupole deformation constants which are to be associated with radii of $r_o = 1.12$ and $r_c = 1.2$, respectively.

	β_N	β_C
^{120}Sn	.13	.112
^{122}Sn	.124	.118

Table II. Two sets of optical model parameters which yield virtually the same
elastic cross section for O + Sn at E = 100 MeV. The optical model radius is
$r_o(A_p^{1/3} + A_T^{1/3})$ and the charge radius is $r_c A_T^{1/3}$.

	V	W	r_o	A	r_c
Becchetti (Ref. 6)	-40	-15	1.31	0.45	1.2
Morrison (Ref. 8)	-100	-40	1.22	0.5	1.2

Figure Captions

Fig. 1. Various routes that can excite the 0^+ and 2^+ states in ^{122}Sn in the
reaction ^{120}Sn(^{18}O,^{16}O)^{122}Sn which are included in the calculation. The
usual DWBA treats only the direct transition from the ground state to each
product state.

Fig. 2. The form factors for two neutron transfer from ^{18}O to ^{120}Sn for the
ground and 2^+ states. The maximum occurs at approximately a separation
distance between O and Sn corresponding to O lying along a radius of Sn.

Fig. 3. Differential cross section in mb./sr. for exciting the ground and 2^+
states in ^{122}Sn, computed in DWBA. Note that the scale is split for the
two levels.

Fig. 4. The coupled channel calculation in which the direct and indirect routes
of Fig. 1 are included in calculating the cross sections are compared with
the direct route alone for the 2^+ state. For the ground, the direct route
is almost the whole contribution so no comparison is shown.

Fig. 5. The effect of varying the collectivity of the inelastic transitions on
the transfer cross sections is shown. The factors correspond roughly to
the amount by which the inelastic cross sections are increased compared to
the normal collectivity of tin.

Fig. 6. Comparison with DWBA when only Coulomb excitation in the inelastic
channels is included. Compare with Fig. 4 to see that nuclear excitation
dominates.

Fig. 7. Fictitious situation with Q of reaction changed from correct value of
2.8 MeV to -6 MeV.

Fig. 8. Comparison of cross sections for two values of reaction Q = ±6 MeV.

Fig. 9.   Comparison of different interference obtained if sign of β_2 is changed.

Fig. 10.   Differential cross sections at 80 MeV are shown.   The direct
contribution to the 2^+ state is shown for comparison.

Fig. 11.   Differential cross sections at 120 MeV.   The jagged peaks at
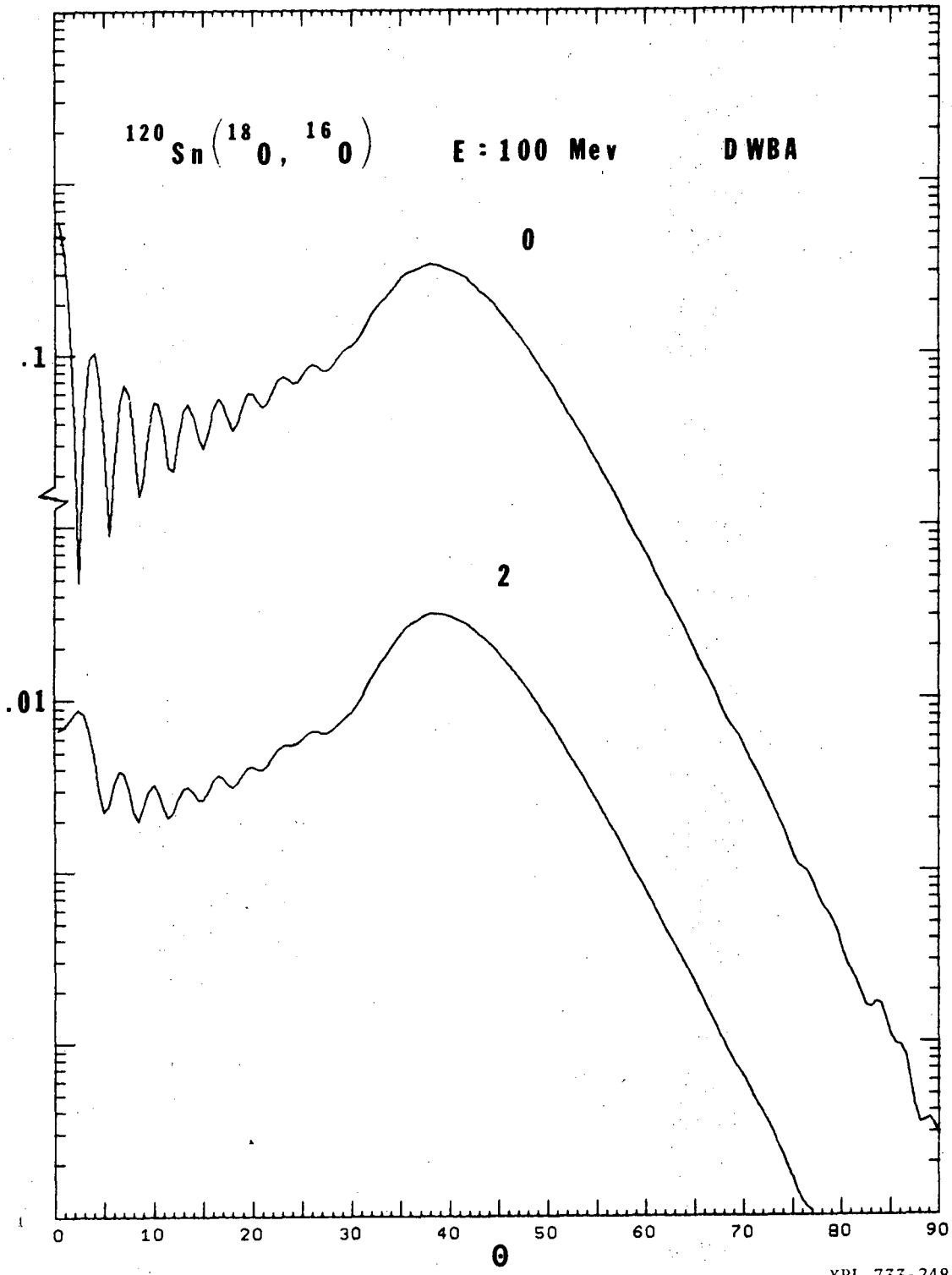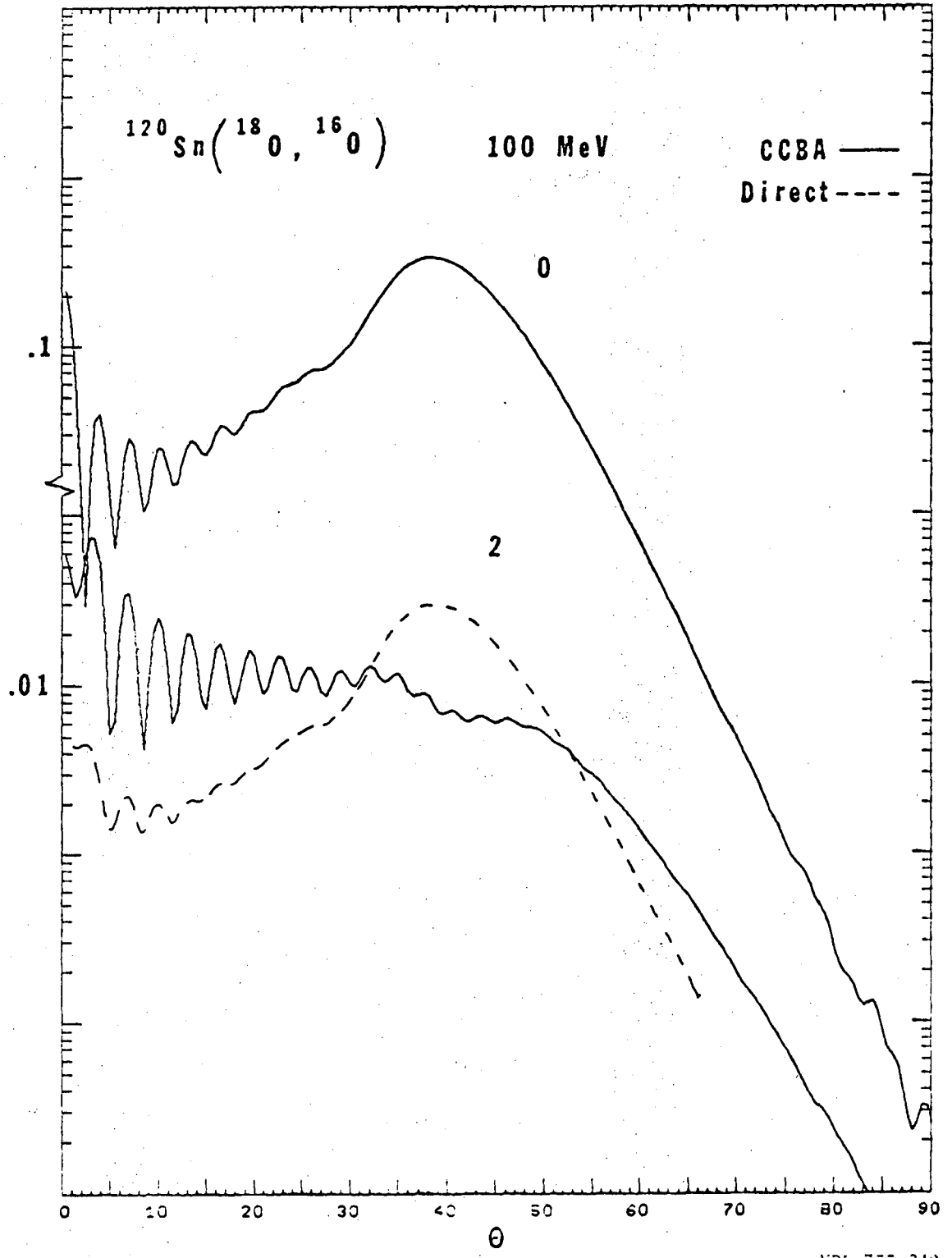$\theta > 60°$ are due to truncation at $\ell = 99$ partial waves.

$^{120}Sn\,(^{18}O,^{16}O)\,^{122}Sn$

Fig. 2

XBL733-2385

$^{120}\text{Sn}\left(^{18}\text{O},\ ^{16}\text{O}\right)$ E : 100 Mev   DWBA

XBL 733-248

Fig. 3

$^{120}Sn\left(^{18}O,^{16}O\right)$ 100 MeV   CCBA ———
Direct ----

XBL 753-249

Fig. 4

$^{120}Sn\left(^{18}O,\,^{16}O\right)$ 100 MeV   CCBA

——— 2 x Collectivity

——— 4 X

······ Normal

Fig. 5

XBL 733-250

XBL 733-251

Fig. 6

$^{120}Sn\left(^{18}O,^{16}O\right)$ 100 MeV

Q = - 6 MeV

CCBA ————
Direct ————

.01

.001

0

2

0

0   10   20   30   40   50   60   70   80   90

0

XBL 733-252

Fig. 7

$^{120}Sn\left(^{18}O,\ ^{16}O\right)$ 100 MeV   CCBA

Fig. 3

XBL 733-253

^{120}Sn(^{18}O, ^{16}O) 100 MeV CCBA

Sign change ——
Normal ··········

Fig. 9

XBL 733-255

$^{120}Sn\left(^{18}O,\ ^{16}O\right)$ 80 MeV CCBA

XBL 733-254

Fig. 10

Fig. 11